10

Two Dimensional Analysis of the Shoulder During a Barrier Side Impact

Tim Walilko, John Cavanaugh, Albert King
Wayne State University

INTRODUCTION

The accurate description of human joint motion is one of the most interesting and challenging areas of impact biomechanics. The description of joint motion is very complicated due to the large number of degrees of freedom and muscles within some joints. Understanding the kinematics of human motion is not only important clinically, but can be used in the development of models simulating human motion under various loading conditions. One of the most severe loading conditions a human can be subjected to is an automobile side impact. The number of fatalities and injuries due to side impact is only second to frontal collisions.[1] The question becomes, how can the occupant of an automobile be protected against possible injury? The shoulder could be a possible mechanism in the protection of the thorax against compressive injuries. To our knowledge, little research has been done in the study of the shoulder's response to impact, specifically lateral loading. High speed film taken of cadavers during blunt lateral impacts reveals that the struck side shoulder "disappears" during impact. By tracking targets on the shoulder complex, and the surrounding regions, it may be possible to explain the motion of the shoulder. Not only can the kinematic motion of the shoulder be determined, but, by incorporating into the analysis the amount of force needed to deflect the shoulder, the energy absorption and stiffness properties of the shoulder can be calculated. The aim of this study is to determine the kinematic motion of the shoulder for unpadded barrier side impacts as well as the stiffness of the shoulder. The study will show that the shoulder does not "disappear" during impact, but is able to absorb some of the energy of the impact. Future analysis may reveal that the shoulder can provide a mechanism in protecting the upper thorax region during a side impact.

BACKGROUND

The shoulder complex has one of the most diverse ranges of motion in the human body. The shoulder complex (Figure 1) consists of four bones (the sternum, clavicle, scapula and humerus) and all of the surrounding muscles.[2] These bones form a support for the shallow ball and socket joint in which the head of the humerus articulates. The shoulder complex is able to move efficiently through at least 11 degrees of motion.[3]

Four major articulations connect the bones of the shoulder complex; the sternoclavicular, scapula-thoracic, acromioclavicular and the glenohumeral joint.[4] The sternoclavicular joint anchors the shoulder complex to the thorax. This joint is the only true connection between the shoulder complex and the thorax. The scapulo-thoracic joint is not a true joint, but allows the scapula to glide on the surface of the thorax. The scapula-thoracic joint consists of the muscles of the upper back holding the scapula in place. The acromioclavicular (AC) joint connects the clavicle to the acromion process of the scapula. This joint is located over the head of the humerus. The glenohumeral joint (shoulder joint) is the a ball and socket joint where the head of the humerus articulates.

With the wide variety of motion, and given the structural complexity of the shoulder, it is very difficult to analyze its passive motion, let alone its motion under an external, laterally applied force. To simulate the kinematic motion, and collect preliminary stiffness properties for the shoulder complex, we used a side-impact sled fixture much like that used at the University of Heidelberg[5].

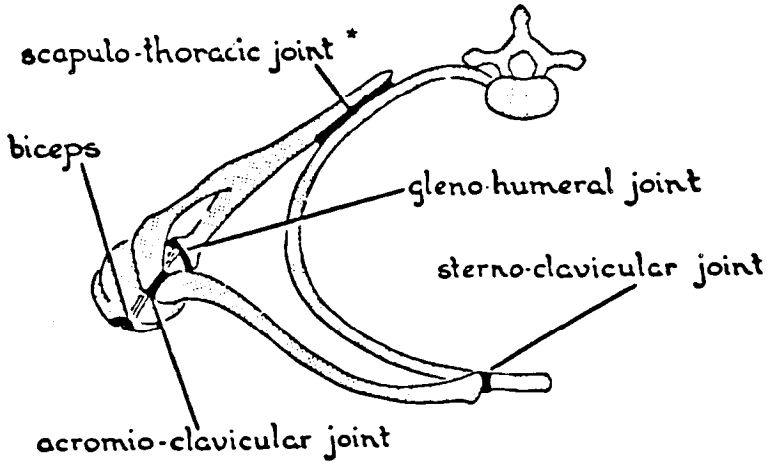

* not a true joint

FIGURE 1: The Shoulder Complex
Reproduced from Bateman, The Shoulder and Neck[6]

METHOD

A Heidelberg-type seat fixture was mounted to a horizontally accelerated sled.[7] The sled was accelerated to velocities of approximately 6.7 and 9.0 m/s, then decelerated within 203 mm, so that the cadaver would continue to slide on a teflon seat into the rigid wall of the seat fixture. The wall was instrumented with nine load cells, two of which were at a 101 x 406 mm beam at the shoulder level. The cadaver was instrumented with accelerometers. Spherical phototargets were rigidly attached to the cadaver for kinematic analysis. The cadavers used in the lateral impacts were unembalmed cadavers donated to the university through the Willed Body Program. The cadaver had X-rays taken, before the run, of all skeletal structures including the shoulder complex.

The region of interest in this study was the section that came in contact with the shoulder beam. This area includes the shoulder complex, the thoracic cage between ribs 1 and 4, and all the internal organs contained within this region.

The cadaver was placed on the Heidelberg-type seat fixture. In order to achieve a lateral impact where the cadaver impacts the wall at the predetermined velocity, the subject was positioned perpendicular and approximately 1 m from the rigid barrier wall, with the left side of the cadaver being the struck side. In all tests, the arms were positioned with the arms slightly anterior to the mid-axillary line. The arms were tied together and placed in the cadaver's lap. Thus, part of the left arm contacted the impact surface.

Post-impact X-rays were taken of all the skeletal structures, including the shoulder. A detailed autopsy was conducted by a board certified pathologist.

Two dimensional kinematic analysis was conducted by tracking the targets relative to a fixed sled reference. Phototargets were rigidly mounted with screws to the upper and lower sternum, left and right acromion joints, left scapula and on the T1 vertebra. Targets were also clamped onto the left clavicle This array of targets were used to measure the upper thoracic deformation, as well as shoulder deflection during impact. The motion was recorded with six high speed cameras with film speeds of 500 to 1000 frames per second. The lateral deflections were measured relative to the front (impacted) edge of the shoulder barrier (Figure 2). The A-P deflections were measured from the upper bar of the seat back which was tangent to the thoracic vertebrae. A-P deflections were actually relative to the thoracic T1 vertebra. The target's position was measured as the perpendicular distance from the center of the target to the plane of the barrier for lateral deflections and from the front edge of the back support for A-P deflections. The deflections were only measured for two dimensional motion. The tracking of the targets was discontinued at the start of rotation of the right shoulder. The start of rotation was estimated by tracking the position of the target at the right AC joint.

POSITIONS OF THE FRAMES OF REFERENCE
USED IN TRACKING THE MOTION
OF THE SHOULDER

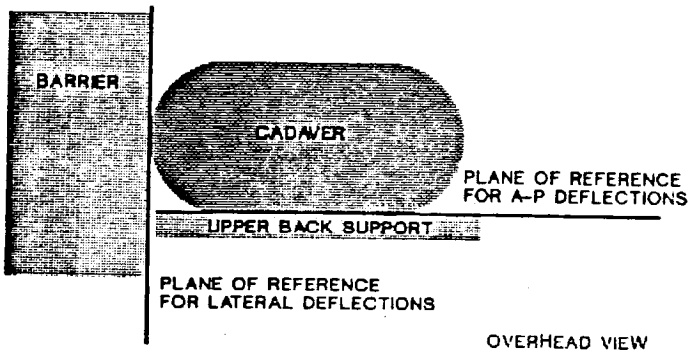

FIGURE 2

Analog data collected from each of the five runs was filtered to SAE channel class 1000 specifications and digitized at 8000 Hz. The digitized data was uploaded for further processing. The force-time curves from the load cells located behind the shoulder barrier were added together to obtain a total force curve for the shoulder region. The force and deflection data was synchronized with the aid of a photoflash. The flash was recorded on film and digitally recorded so that the two could be aligned. The electrical circuit was completed when the shoulder came in contact with the barrier. All digitized data was digitally filtered at 300 Hz with a four pole, phaseless algorithm before being analyzed.

The data was normalized using Mertz's procedure for normalizing impact response data.[8] The method models the torso as a simple mass-spring system of effective mass (Me) and stiffness (K). The displacement, velocity, and acceleration of the mass can be expressed by the differential equations of motion.

The effective mass can be calculated by an impulse-momentum analysis of a free body diagram of the cadaver. Using the model of a simple mass-spring system the impulse-momentum equation simplifies to:

$$M_e = \frac{\int F dt}{Gt + V_o}$$

For the Heidelberg-type test setup, the cadaver is translating on the seat pan at approximately a constant velocity, so the acceleration (G term) dropped out of the equation. The data was normalized to a 50th percentile male (M_e=76 Kg)[9]. The normalization factor for mass is as followed:

$$R_M = \frac{M_S}{M_E}$$

The stiffness term (K) of the simple spring-mass system, can be derived as a function of the structure's geometry (L) and modulus of elasticity (E). For geometrically similar shapes, the stiffness equation takes the form:

$$K_1 = C_1 L_1^a E_1^b$$

where C is a constant which is the same for geometrically similar shapes. Analyzing the above equation, it can see that for dimensional consistency, **a** and **b** must be equal to **1**. **L** is the length factor, which in these tests, is the biacromial shoulder breath. The shoulder breath (L_S) of a 50th percentile male is 398.78 mm[9]. The equation further simplifies by assuming that the elastic modulus to be the same for all cadavers. Although all cadavers may have approximately the same modulus, no two cadavers have the same shape so no two cadavers have the same C_l term. The normalization factor for shape will only account for geometric changes on the impacted side, since only one side of the cadaver is impacted. The diameter of the biceps was used as a normalization factor for shape since the arm was part of the impact surface. So the C_l term became the diameter of the biceps. The diameter of the cadavers biceps was measured by dividing the circumference by π. The circumference used to normalize the data was 307.34 mm, the biceps circumference of a 50th percentile male[9]. The normalization factor for stiffness is:

$$R_K = \frac{K_S}{K_i}$$

Solving the differential equation of motion for the simple spring-mass system in terms of mass and stiffness indicates the displacement can be expressed by:

$$X = V_i \sqrt{\frac{M_e}{K_i}} SIN\left(\frac{K_i}{M_e} t\right)$$

where V_i is the sled velocity. The velocity and acceleration equations can be obtained by taking the derivative of the displacement equation. The magnitude of the force, **F**, acting on the mass during impact is proportional to the deflection of the spring times the springs stiffness and can be expressed by multiplying the stiffness term times the displacement equation. Comparing the experimental parameters to that of a standard test subject, and by substituting in the mass and stiffness normalization factors, we obtain the following normalization factors:

$$R_f = \frac{V_s}{V_i}\sqrt{R_m \times R_k} \qquad R_a = \frac{V_s}{V_i}\sqrt{\frac{R_k}{R_m}} \qquad R_v = \frac{V_s}{V_i} \qquad R_x = \frac{V_s}{V_i}\sqrt{\frac{R_m}{R_k}}$$

subscript: **s**=standard test subject
i=individual test subject

V_S=standardized sled velocity (6.7 or 9 m/s)
V_i=sled velocity of individual test

R_f, R_a, R_v and R_x are the normalization factors for force, acceleration, velocity and displacement, respectively based on the physical characteristics of the 50th percentile male. The normalization factors take into account many variables such as small changes in velocity and changes in the shape and mass of each cadaver.

RESULTS

Test parameters for the five runs are summarized in Table 1. The cadavers ranged in age from 60 to 69 years, with an average age of 65. The test subjects consisted of one female and four male subjects. The five cadavers had an average mass of 62.3 kg and an average height of 1.70 m. The tests were conducted at sled velocities close to 6.7 or 9.0 m/s, although the actual velocity of the cadaver at barrier impact varied slightly from the sled velocity.

SUMMARY OF SIDE IMP/ :T TEST PARAMETERS

RUN NO	VEL (M/S)	CADAVER NO	ASS KG)	HEIGHT (M)	AGE	SEX
RUN-04	9.05	215	57.6	1.63	69	M
RUN-05	6.71	216	14.0	1.72	67	M
RUN-06	9.04	217	51.2	1.84	60	M
RUN-07	6.67	206	74.8	1.70	66	M
RUN-08	6.59	UM12	73.9	1.62	64	F

TAB E 1

A summary of the injuries occurring in thi: egion are presented in Table 2. All of the runs resulted in seven to eight fractures of the left side s 1 to 4. The prominent injuries in the shoulder complex were, separation of the acromioclavicular int and fractures of the acromion process at the accelerometer mount site. The AC joint separation i: clinically seen injury and is described in detail by Moore.[10] The acromion fracture has not been ob rved clinically and may be an artifact of the test. In the single female cadaver run (RUN-8), there occ red more injuries than in the four male subjects.

SHOULDER IN RY SUMMARY

RUN NO.	INJUR	NO. OF LEFT SIDE RIB FRACTURES (RIBS 1-4)
RUN-04	Fx. of Acromior Process Separation of C Joint	7
RUN-05	No Injur	8
RUN-06	Fx. of Acromior Process Separation of C Joint	7
RUN-07	Fx. of Acromior Process Separation of C Joint	7
RUN-08	Separation of C Joint Fx. of Cla le Fx. of Ste m	8

TAE E 2

The following data analysis focuses on the comparison between RUNS 5 and 7. The significance of these two runs is that one run had an AC joint separation (RUN-7), and the other run had no AC joint separation (RUN-5). These runs were conducted at approximately the same sled velocity of 6.7 m/s. The data from the remaining runs are added for completeness and are summarized in Tables 3 and 4. These data are also presented as Figures in the Appendix. Some of the data is missing in Tables 3 and 4 due to the unavailability of the rear camera in RUN-8. Also, in some runs, the head obstructed the view of certain targets so they could no longer be tracked from a given camera position.

In the comparison between RUNS 5 and 7, it can be seen from Table 3 and Figures A1, A3 and A8 that the lateral deflections are consistently smaller in RUN-5 where no AC joint separation was observed, as compared to RUN-7 with AC separation. One can also observe, when comparing the sternal A-P deflections that the sternum moves anteriorly, away from the spine, as the sternum approaches the barrier. The scapula deflects posteriorly as well as medially, from its initial position at shoulder contact. In RUN 7, the scapula does not appear to deflect posteriorly nearly as much as when the AC joint remained intact in RUN 5.

MAXIMUM SHOULDER DEFLECTION
DATA SUMMARY

RUN NO.	T1	STERNUM		SCAPULA	
	(LAT.)	(LAT)	(A-P)	(LAT)	(A-P)
RUN-04	83.1	168.1	45.0	54.1	--
RUN-05	78.9	79.4	37.1	65.7	34.7
RUN-06	112.3	65.2	--	66.3	--
RUN-07	134.6	131.9	--	109.3	33.7
RUN-08	--	131.9	--	90.1	--

Deflections in mm

TABLE 3

In the comparison of the force-time histories, it can be observed that the force peaks at an average value of 4032 N for the 6.7 m/s sled velocity. For the 9.0 m/s, runs the forces peaked at average of 6180 N.

The force-deflection histories presented in Figures A12 and A13 are cross plots of the total force measured at the shoulder barrier and the deflection of the T1 spinal target, relative to the barrier. Thus the force-deflections shown are actually half upper thorax force-deflections, which is a composite of the thoracic cage and the shoulder complex force-deflections. Table 4 shows that the deflections are smaller in RUN-5 as compared to RUN-7. The initial stiffness of the half thorax was also tabulated by calculating the slope of the rising section of the force-deflection curves. Note in Table 4 that the initial stiffness of the half thorax is four times greater in RUN-5 than in RUN-7. The stiffness in RUN-5 may be much greater because the AC joint remained intact. Table 4 also contains the amount of energy stored in the half thorax during linear compression. This was calculated by finding the area under the force-deflection curves. The stored energy is greater in the intact AC joint run, then in separated AC joint run.

FORCE-DEFLECTION
DATA SUMMARY

RUN NO.	FORCE (N)	DEFLECTION (mm)	STIFFNESS (N/mm)	ENERGY STORED (J)
RUN-04	6153	83.1	139	292
RUN-05	4206	78.9	228	206
RUN-06	6207	112.3	156	302
RUN-07	3858	134.6	70	124

TABLE 4

The data is Table 3 is relative to a fixed sled reference. The data in Figures A14-A17 considers how the various components move relative to each other. It can be seen that both the upper and lower sternum target positions have approximately the same time histories (Figure A14 and A15), so that there is minimal rotation of the sternum in the frontal plane. In comparing the T1 and sternum targets (Figures A16 and A17), it can be seen that right after initial shoulder contact the sternum appears to rotate clockwise with respect to T1 (looking from overhead) but, as the upper thorax approaches maximum compression the sternum rotates back, counterclockwise, towards the barrier. With the AC joint intact (RUN-5), this initial thorax rotation seems to be more restricted than in runs with AC joint separation.

DISCUSSION

Shoulder motion, presented in Figures 3 and 4 is based on the film analysis of RUNS 5 and 7. These figures show the approximate position of the various links at shoulder contact and at maximum deflection of the T1 spinal target. The initial shoulder position at shoulder contact is shown in black with the center of the AC joint approximately 6 cm away from the barrier. This is to account for any soft tissue of the deltoid and upper arm. The position of the shoulder at maximum compression is shown in gray.

The bones of the shoulder complex are assumed not to fracture, but to act as rigid links. The ribs are added to illustrate maximum thoracic compression. The ribs are assumed not to break. In actual tests rib fractures occurred. The acromioclavicular and sternoclavicular joint are modeled as simple hinges. The model assumes the motion of the shoulder is confined to a single plane with no inferior-superior motion.

For the intact AC joint (RUN-5), the AC joint moved towards the barrier and posteriorly with respect to its original position at shoulder contact. Compare this to Figure 4 where the AC joint appeared to translate towards the wall with no A-P motion. The scapula appeared to rotate clockwise about the AC joint by the compression of the ribs and soft tissue. The sternum (shown in Figures 3 and 4) appeared to move laterally towards the wall, and anteriorly with respect to its initial position.

The combination of the AC joint translation into the barrier and the scissoring motion of the clavicle and scapula may be the reason for the increase in stiffness and amount of energy stored in the intact shoulder complex. The scissoring motion of the shoulder can be represented by a torsional spring and the linear translation as a linear spring. The increase in stiffness may also be due to the rotation restrictions that the shoulder complex puts on the thorax since it is easier to rotate the thorax out of the way than to laterally compress it. This increase in stiffness is important to note, because by increasing the stiffness, less deflection is needed to store the same amount of energy. Note the amount of extra rib deflection when the AC joint fails (RUNS 7). With less deflection, there is less of a chance of compression related injuries.

Figures 3 and 4 present an overall picture of shoulder compression in lateral impact based on results obtained through film analysis, but the model has some shortcomings. The model assumes the scapula, clavicle and sternum never lose contact with each other, but by the time the bones reach

OVERHEAD VIEW OF SHOULDER DURING LATERAL LOADING

(ACROMIOCLAVICULAR JOINT INTACT)

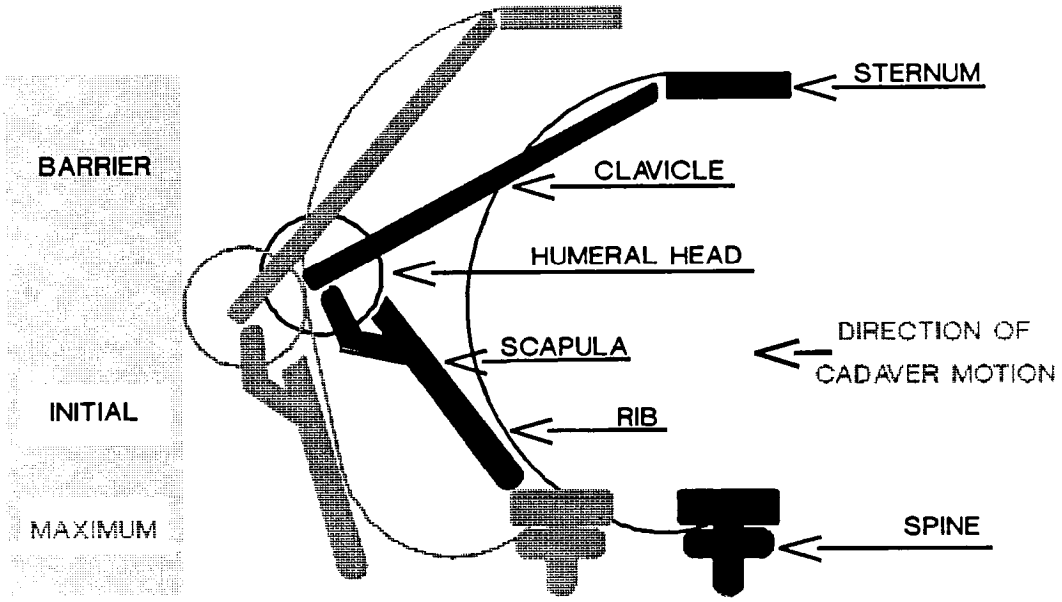

FIGURE 3

(ACROMIOCLAVICULAR JOINT SEPARATION)

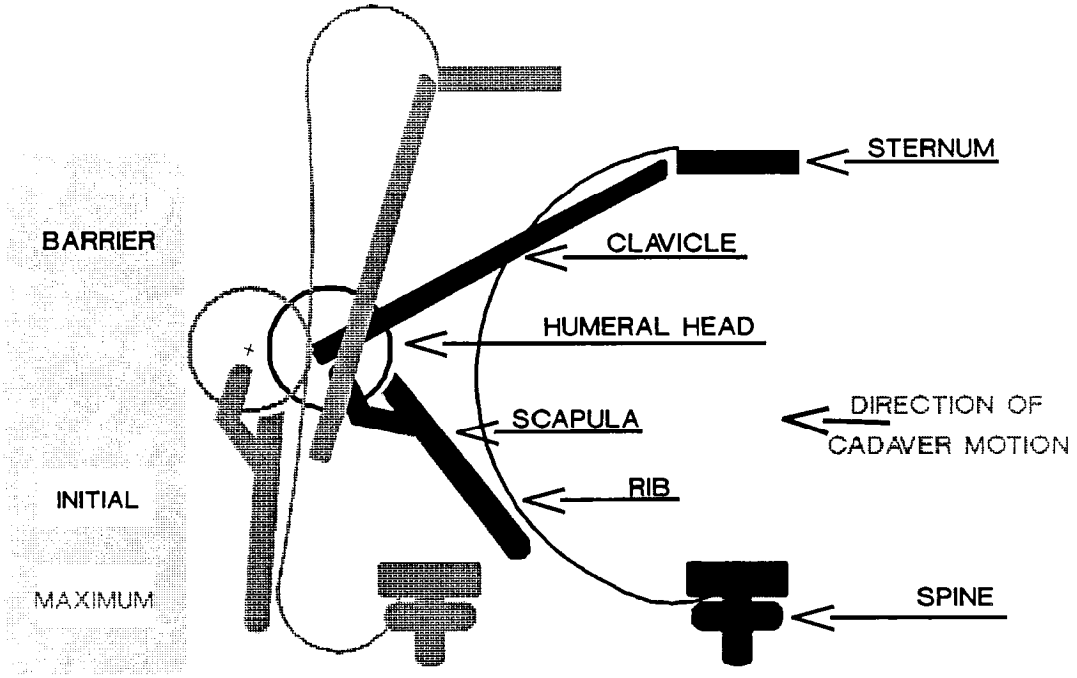

FIGURE 4

maximum compression they have separated from each other. If the bones do not elongate during impact, the extra deflection might come from the stretching of the ligaments within the joints. This is supported by a graphical analysis of RUN-5 which showed that the total separation between the clavicle and scapula and between the clavicle and sternum added approximately 10 mm to the A-P deflection.

CONCLUSION

The data analyzed from the five rigid wall tests show that there may be a connection between AC joint separation and the amount of lateral thorax deflection. With the shoulder intact, the deflections of the sternum, scapula and T1 are decreased. The data shows that the shoulder "scissors" about the AC joint, which appears to absorb some of the energy of the impact. The shoulder also appears to restrict the rotation of the upper thorax. To verify this rotation, a three dimensional analysis will be conducted. The combination of the scissoring motion of the clavicle and scapula and the decrease in thorax rotation may increase the stiffness of the upper thorax. The increase in stiffness may be important in the prevention of compression related injuries, because as the stiffness is increased, less compression is needed to absorb the same amount of energy. Although the shoulder appears to absorb some of the energy of the impact, the shoulder's ability to prevent injury is still speculation, since all of the cadavers suffered numerous rib fractures. The data suggests that the shoulder is an energy absorbing mechanism.

ACKNOWLEDGMENTS

This work is supported by CDC Grant No. CCR 502347. We wish to thank Frank DuPont, Pradeep Balakrishnan, Mark Libich, Warren Hardy, Jim Kopacz and the rest of the Wayne State Bioengineering Center staff who were an integral part of this study. We also wish to acknowledge Dr. Kurtzman for performing the autopsies and for providing valuable insight into the injuries which occurred. We wish to thank Jiff Marcus and Rolf Eppinger of NHTSA for their cooperation and input into this project.

REFERENCES

1. D.C. Viano and C.C. Culver, L. Evans, M. Frick, and R. Scott, "Involvement of older drivers in multi-vehicle side impact crashes", Proc. 33rd Annual Proc. AAAM, 1989.

2. A.E. Engin and R.D. Peindl, "On the biomechanics of human shoulder complex-I. kinematics for determination of the shoulder complex sinus", J. Biomechanics, Vol 20, No 2, pp.103-117, 1987.

3. A.M. Cook, "Electrically-controlled upper extremity amputees using myoelectric and conventional prostheses", Electronic Devices for Rehabilitation, Webster, Cook, Tompkins and Vanderheiden, eds. New York: John Wiley & sons, 1985.

4. H. Gray, Grays Anatomy 29th American Edn, C.M. Goss. ed, Philadelphia: Lea & Febiger, 1973, pp. 317-326.

5. J.H. Marcus, R.M. Morgan, R.H. Eppinger, D. Kallieris, R. Mattern, and G.Schmidt, "Human response to injury from lateral impacts", SAE Paper No 831877, 27th Stapp Crash Car Conference, 1983.

6. J.E. Bateman, The Shoulder and Neck, Philadelpia, W.B. Saunders Co., 1972, p. 139.

7. J. Cavanaugh, T. Walilko, A. Malhotra Y. Zhu and A. King, "Biomechanical response and injury tolerance of the thorax in twelve sled side impacts", SAE Paper No. 902307, 34th Stapp Car Crash Conference Proceedings, 1990.

8. H.J. Mertz, "A procedure for normalizing impact response data", SAE Paper No. 840884, Government/Industry Meeting & Exposition, Washington D.C., 1984.

9. E. Churchill, T. Churchill, K. Downing, ed., Anthropometric Source Book Volume II: A Handbook of Anthropometric Data, NASA Reference Publication 1024, July 1978.

10. K.L. Moore, Clinically Oriented Anatomy, Baltimore, The Williams and Wilkins Co., 1980, pp. 810-847.

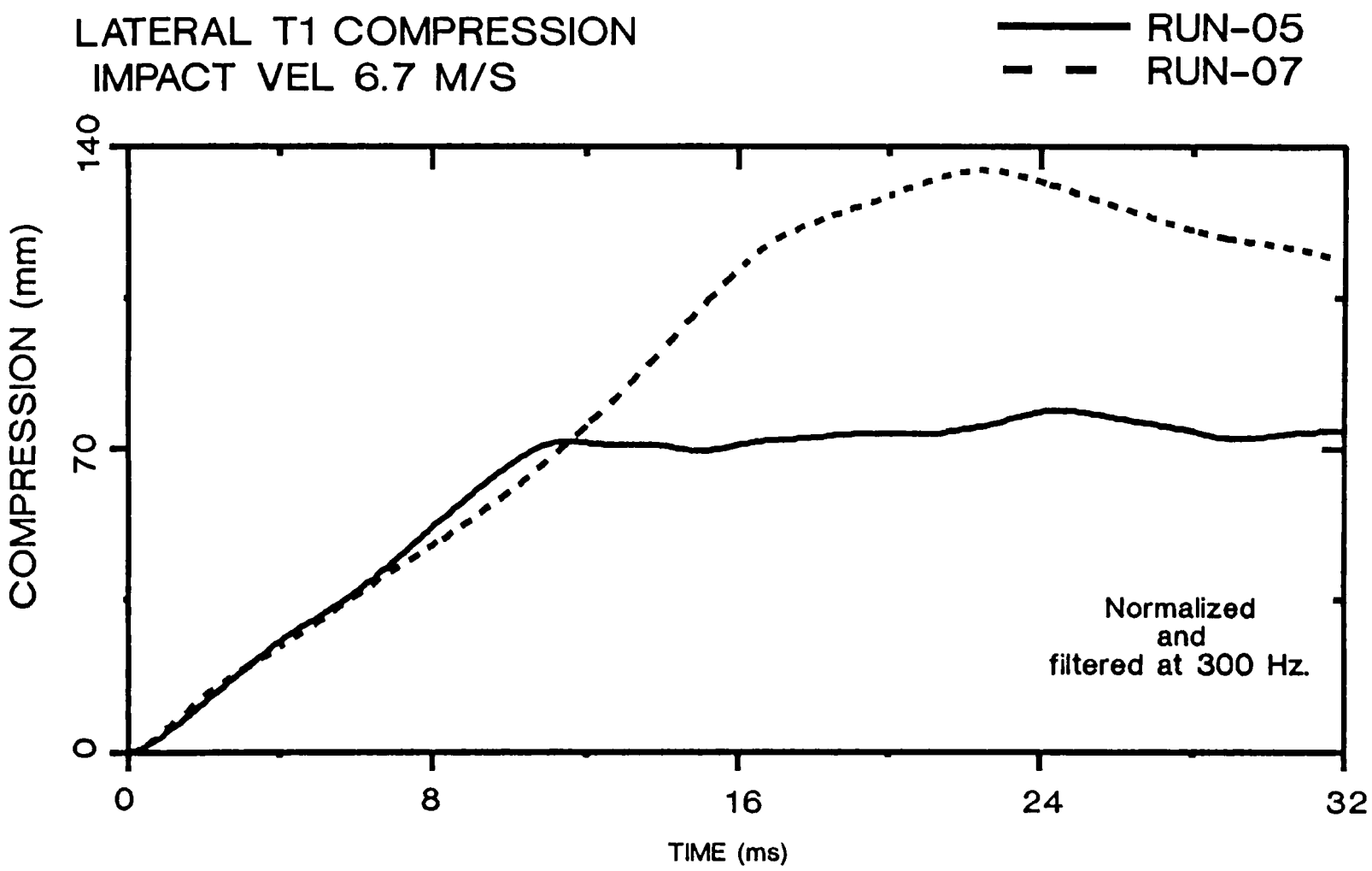

Wayne State University
Bioengineering Center

FIGURE A1

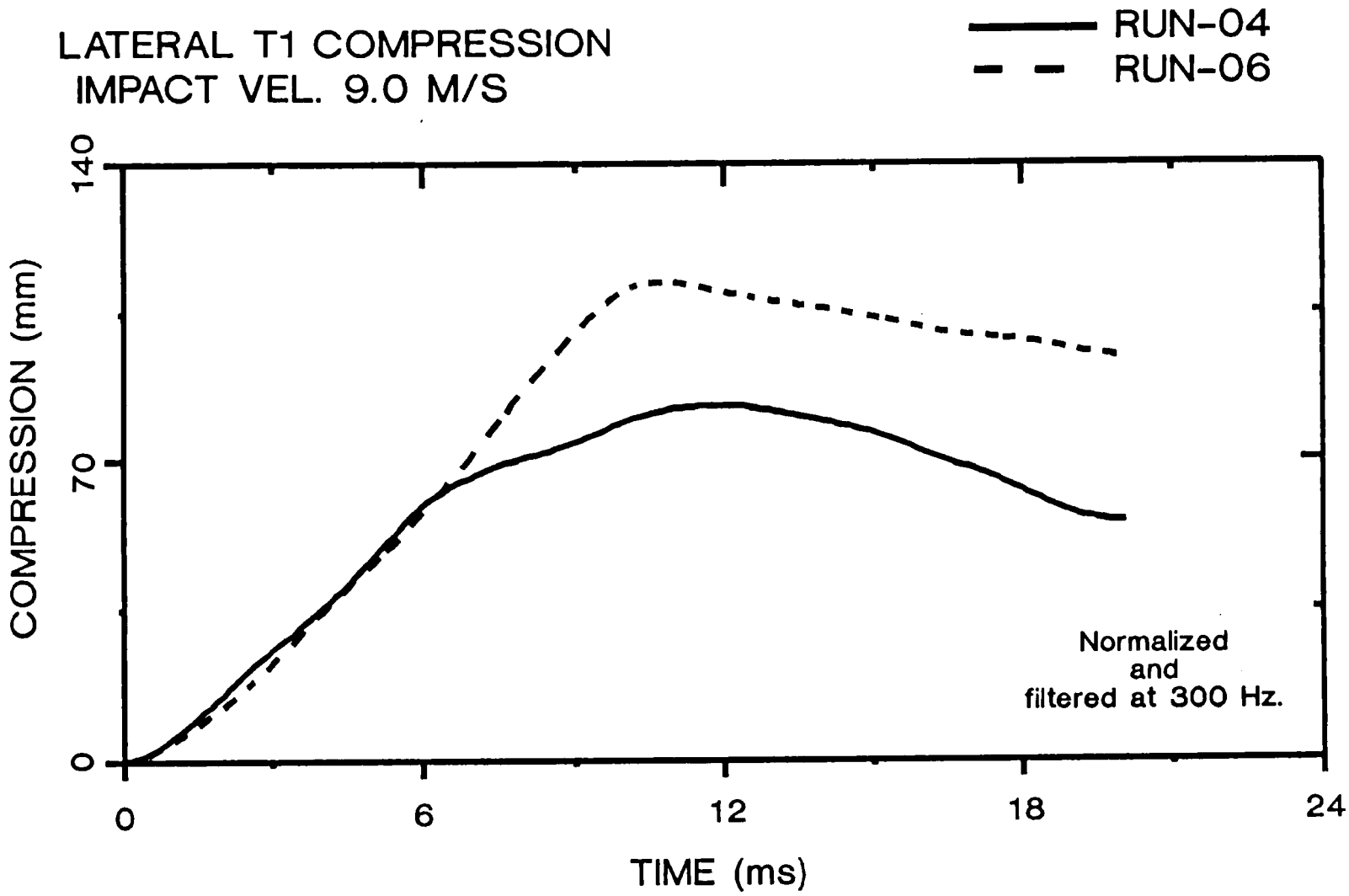

Wayne State University
Bioengineering Center

FIGURE A2

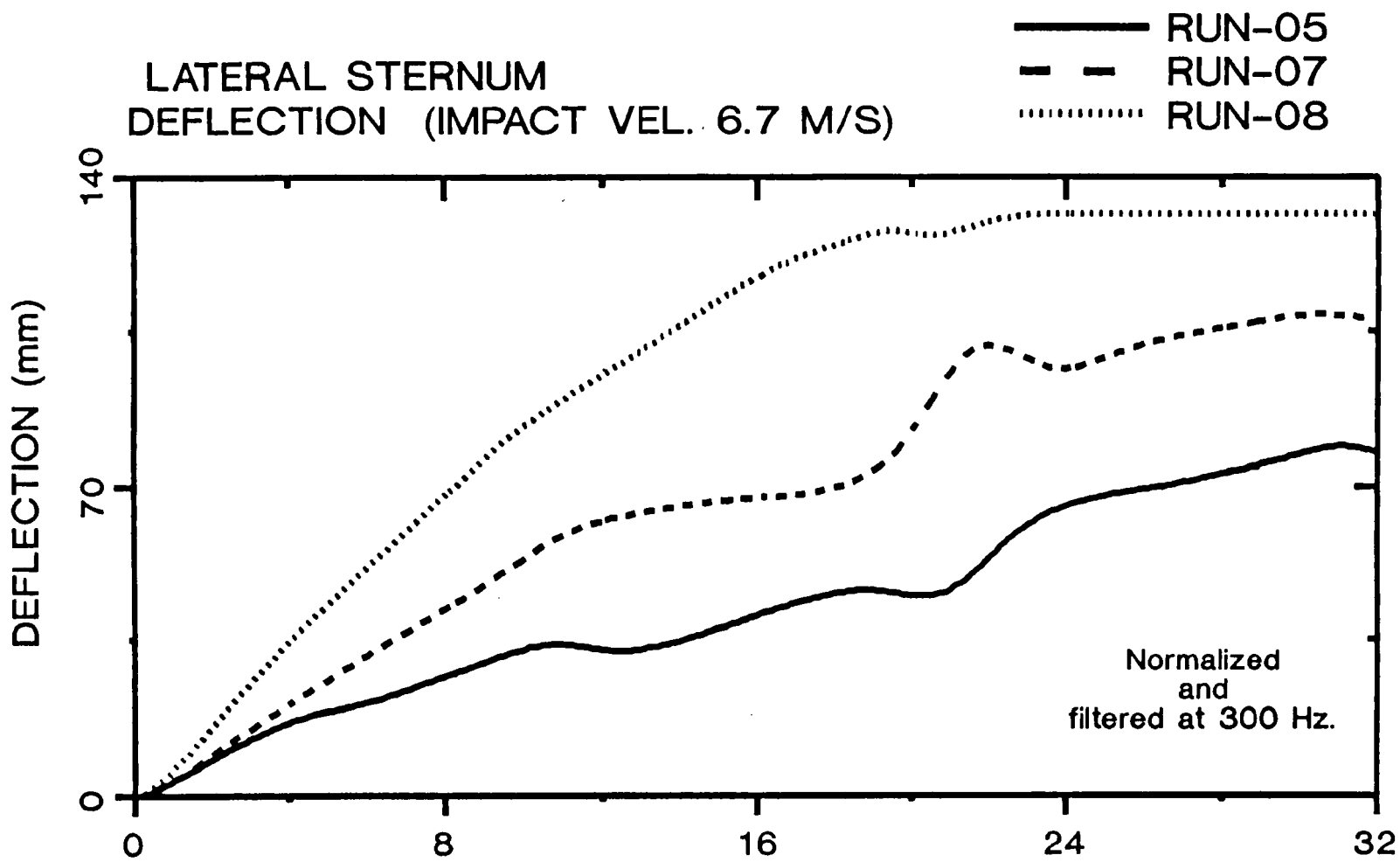

Wayne State University
Bioengineering Center

FIGURE A3

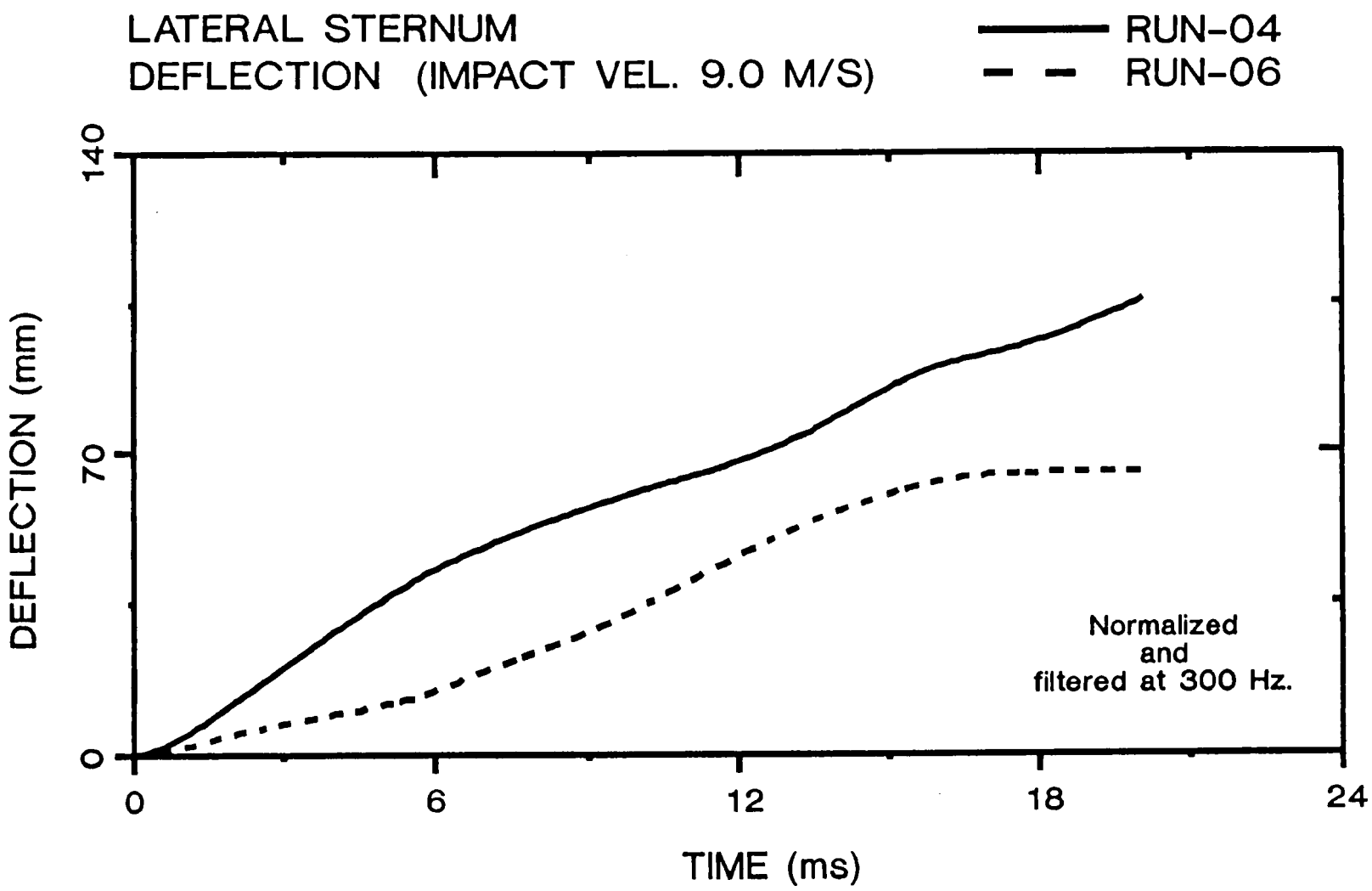

Wayne State University
Bioengineering Center

FIGURE A4

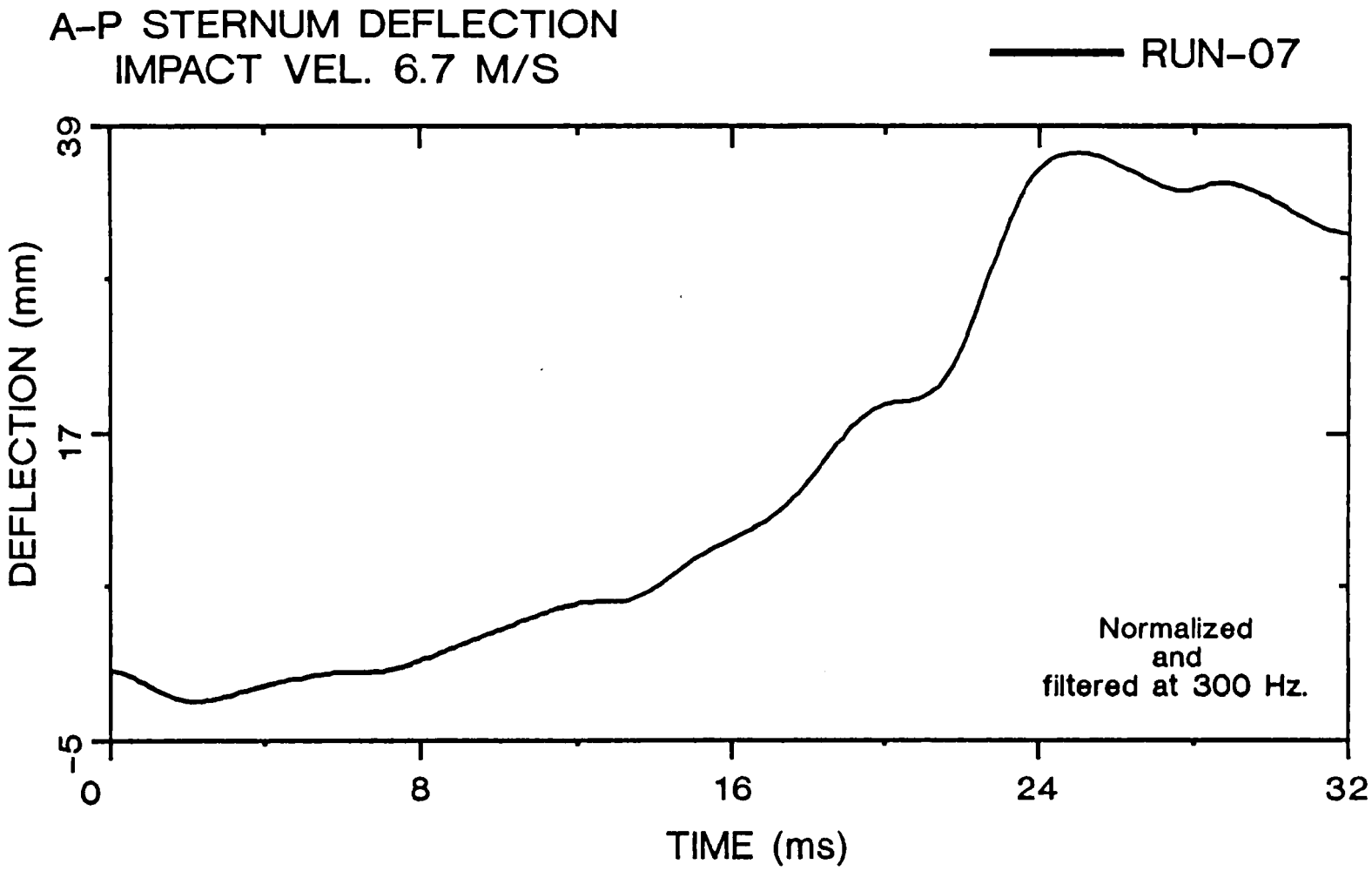

Wayne State University
Bioengineering Center

FIGURE A5

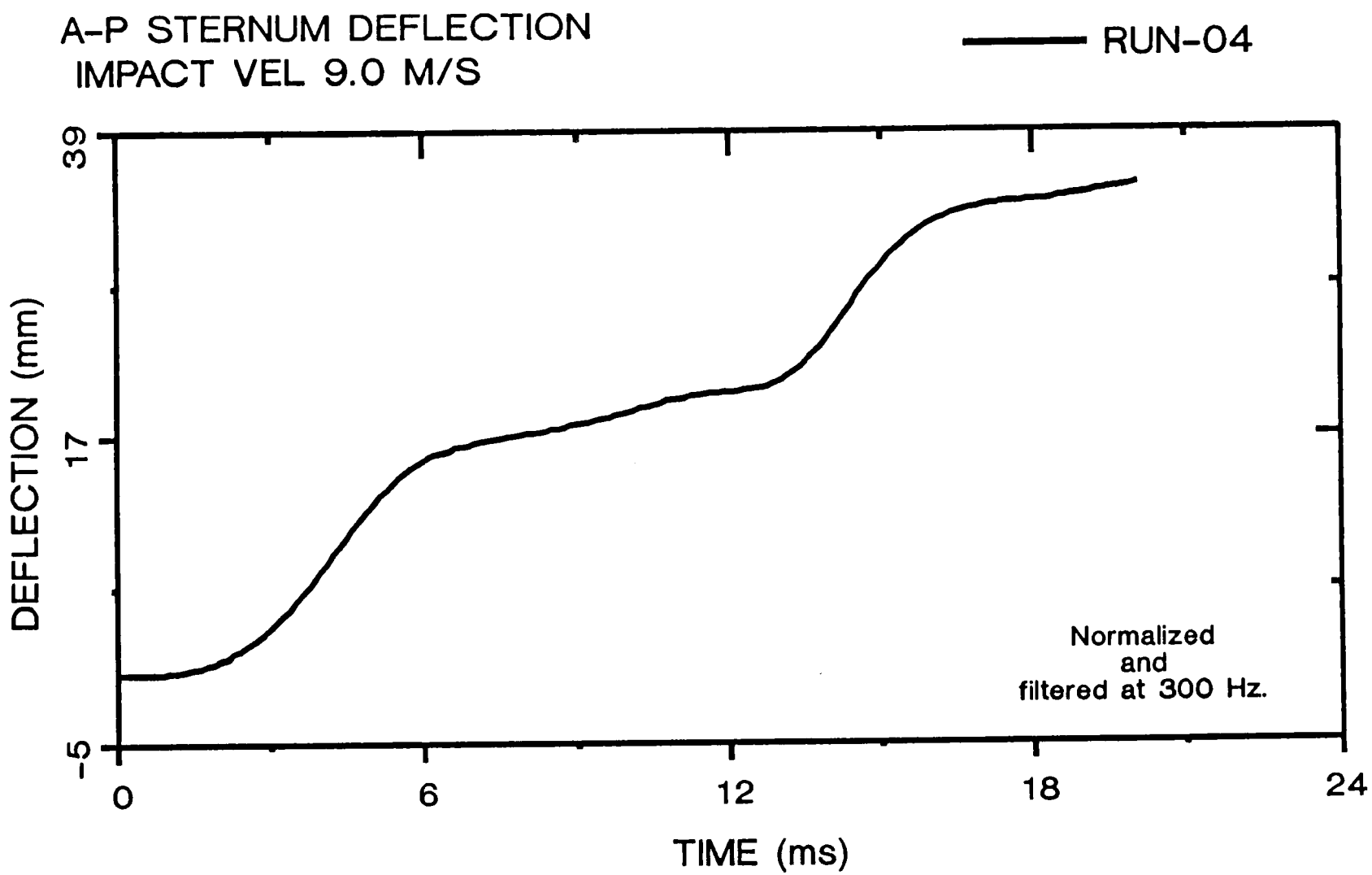

Wayne State University
Bioengineering Center

FIGURE A6

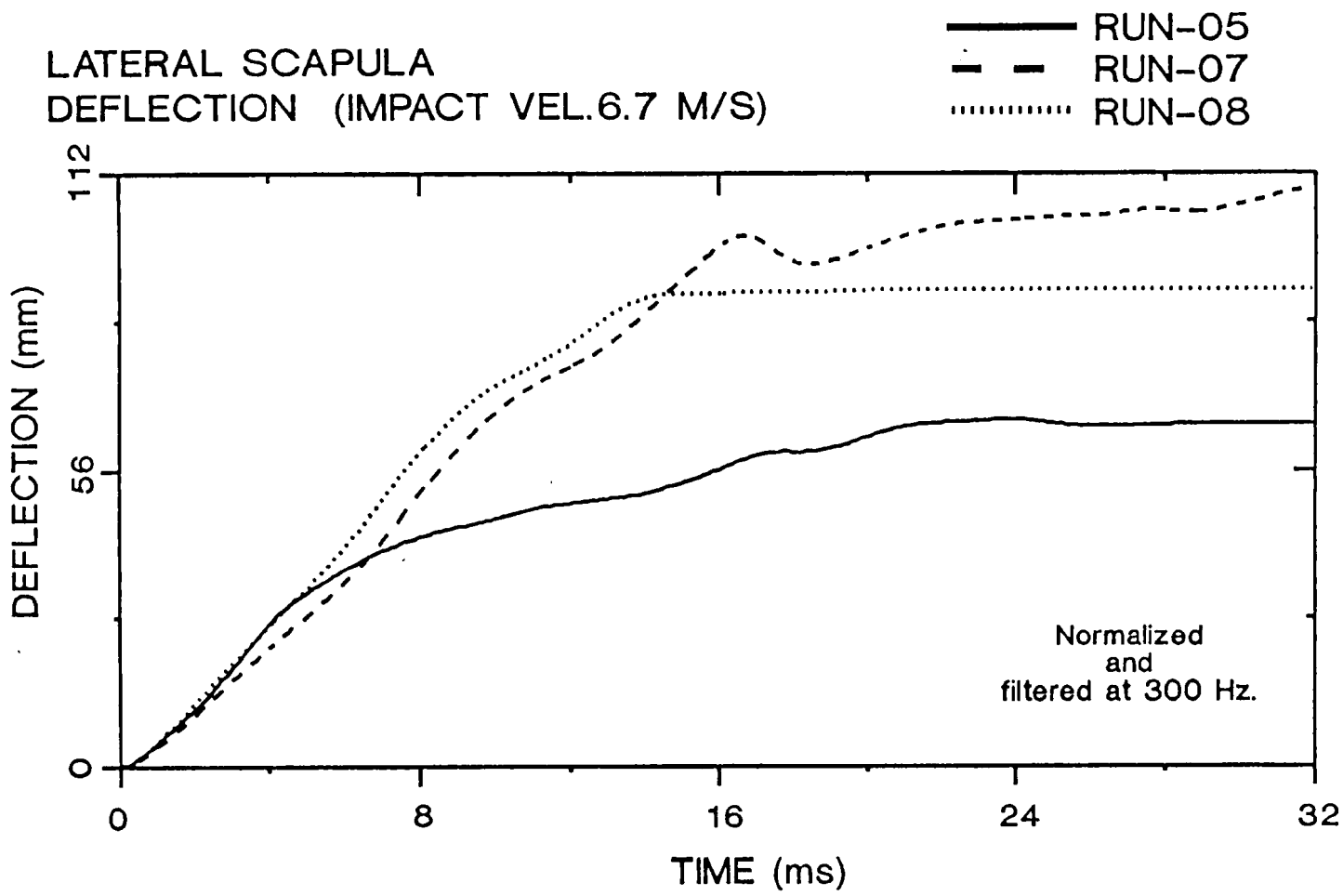

Wayne State University
Bioengineering Center

FIGURE A7

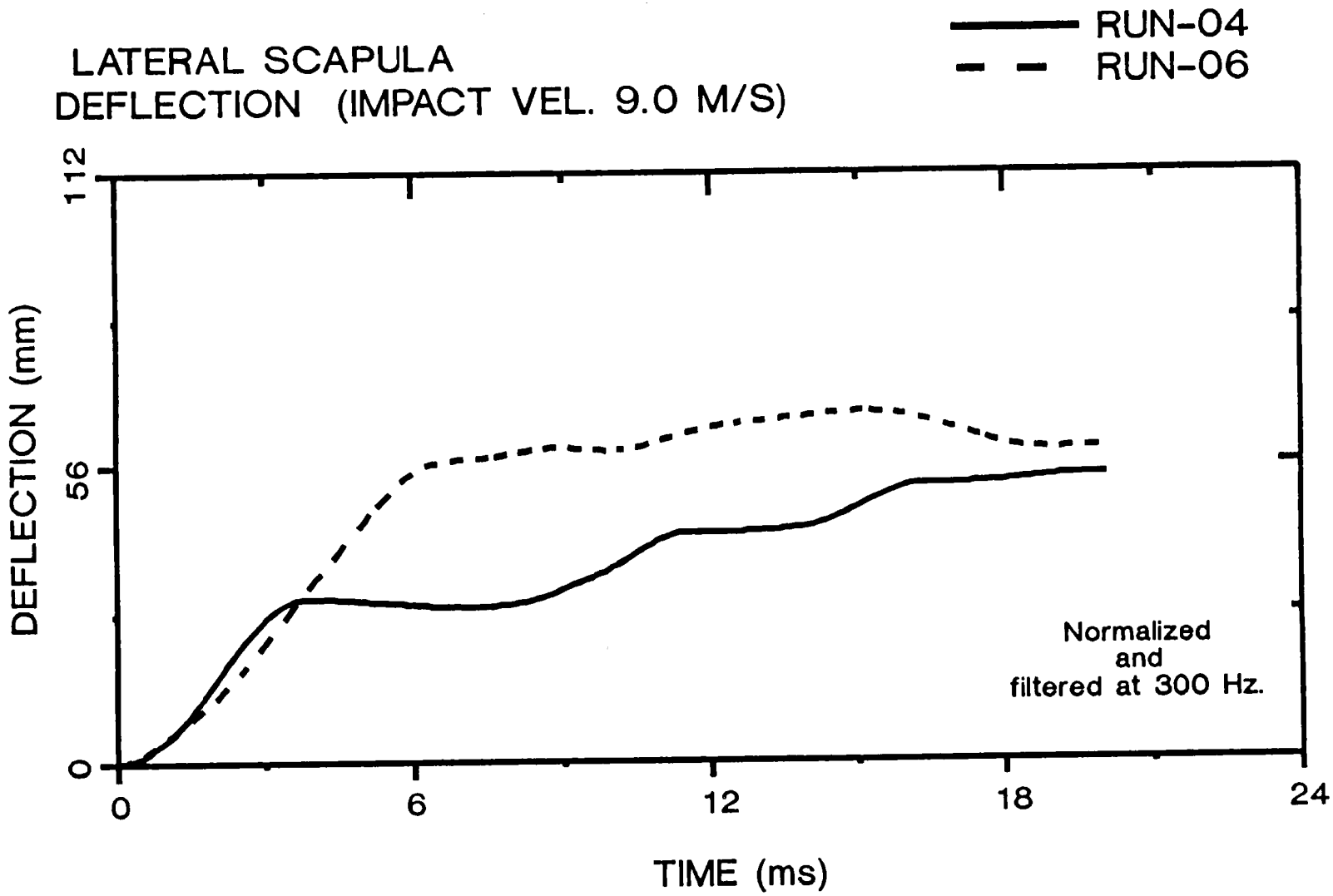

Wayne State University
Bioengineering Center

FIGURE A8

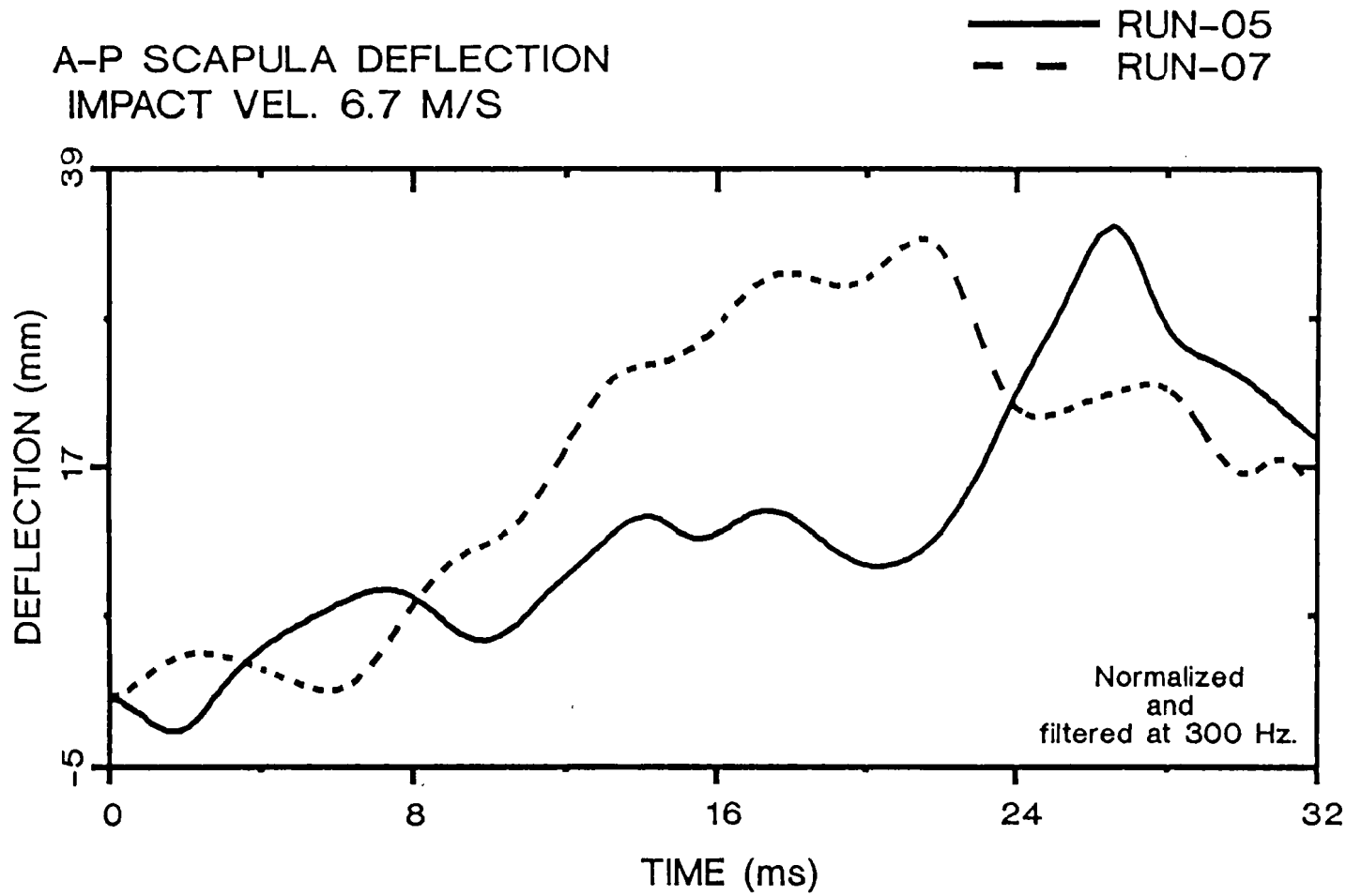

Wayne State University
Bioengineering Center

FIGURE A9

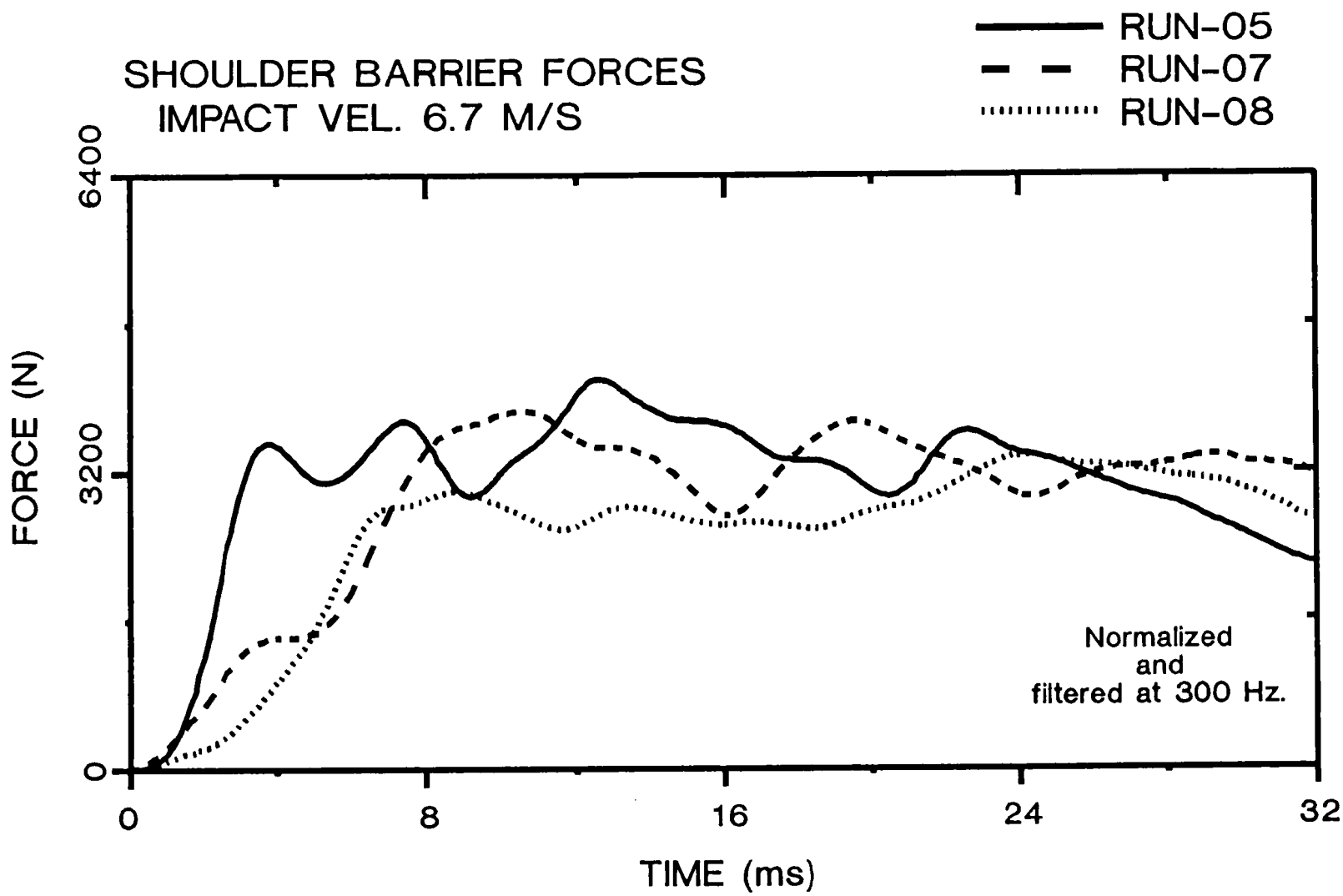

Wayne State University
Bioengineering Center

FIGURE A10

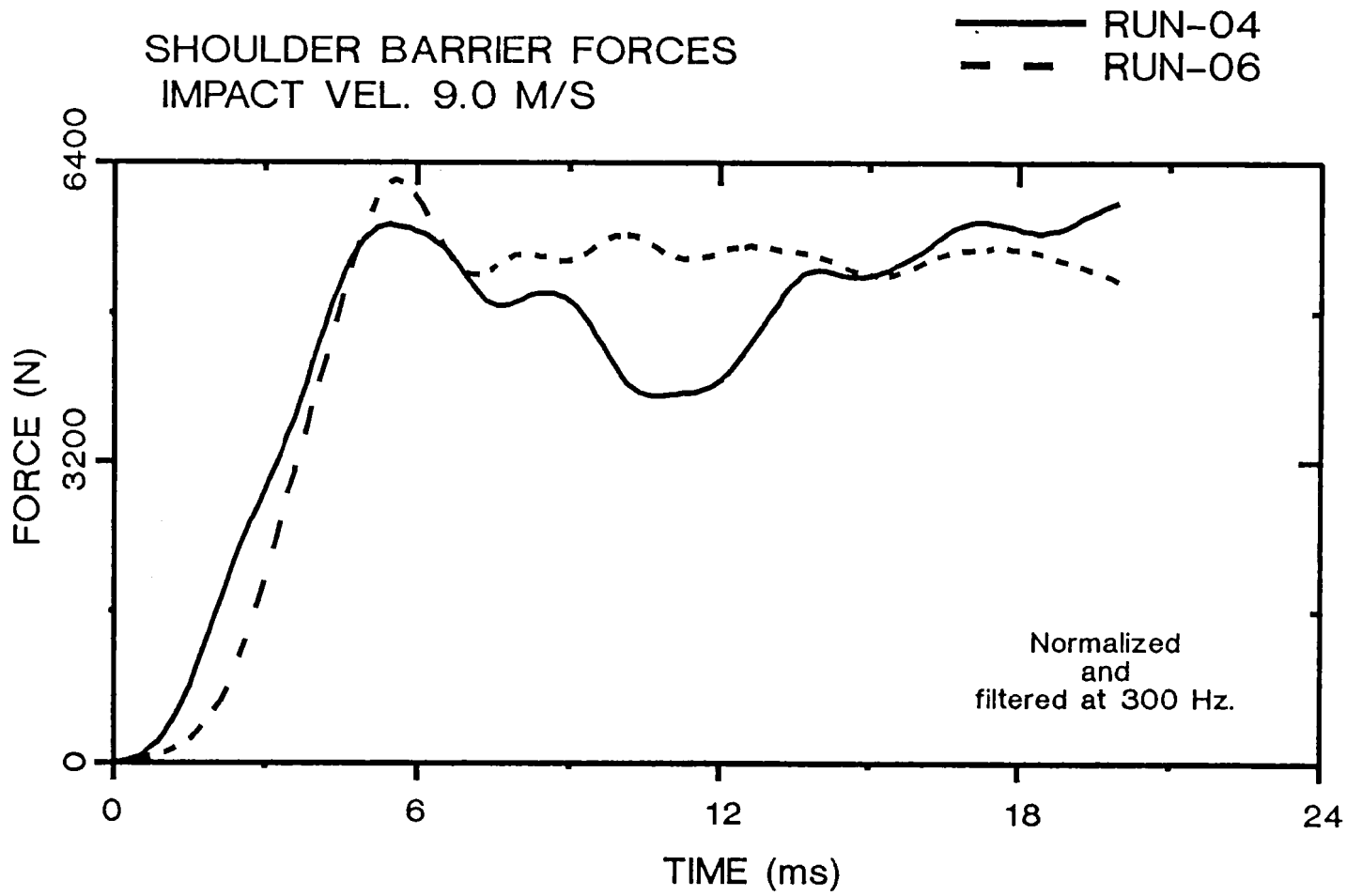

Wayne State University
Bioengineering Center

FIGURE A11

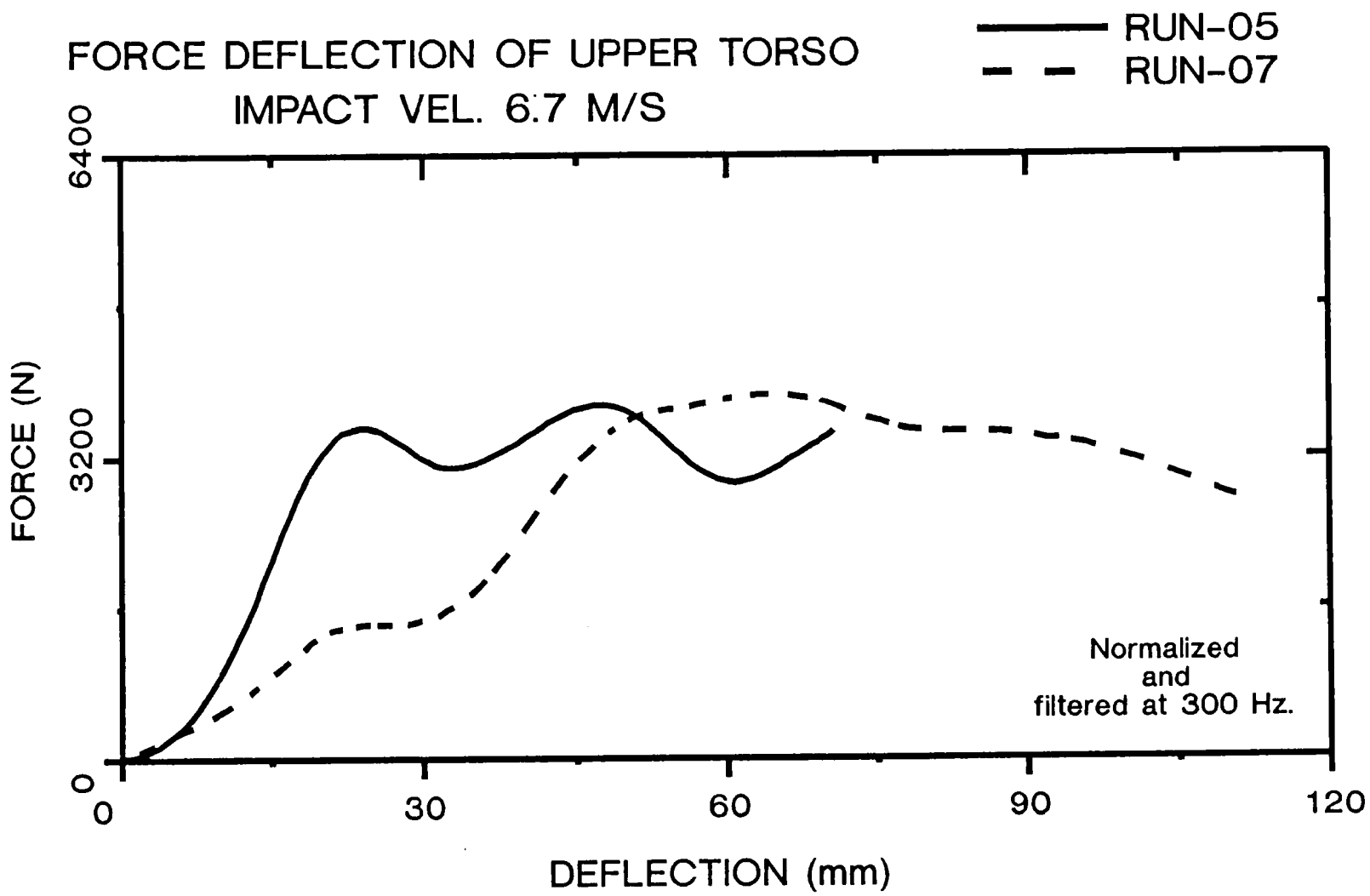

Wayne State University
Bioengineering Center

FIGURE A12

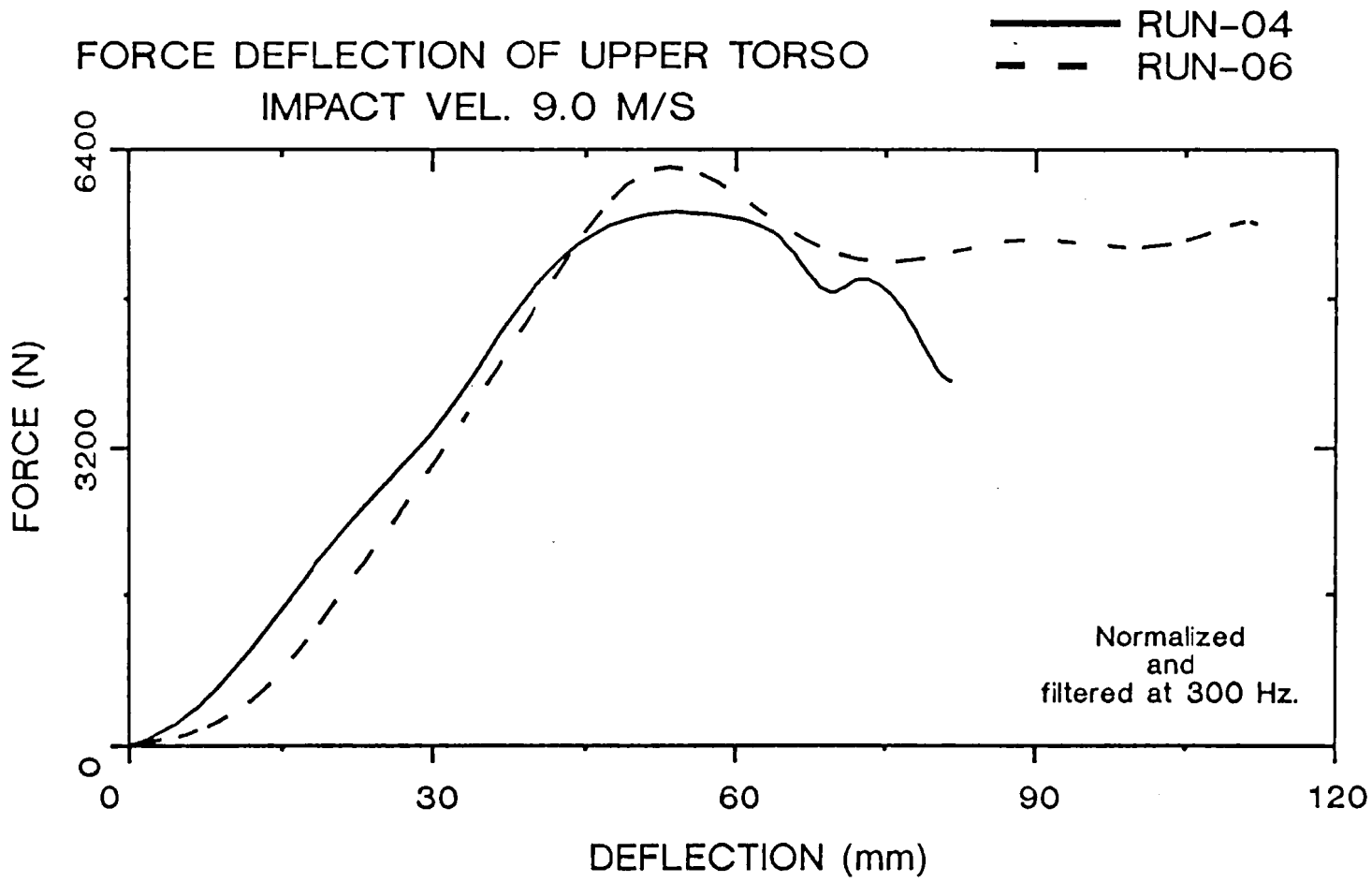

FIGURE A13

Wayne State University
Bioengineering Center

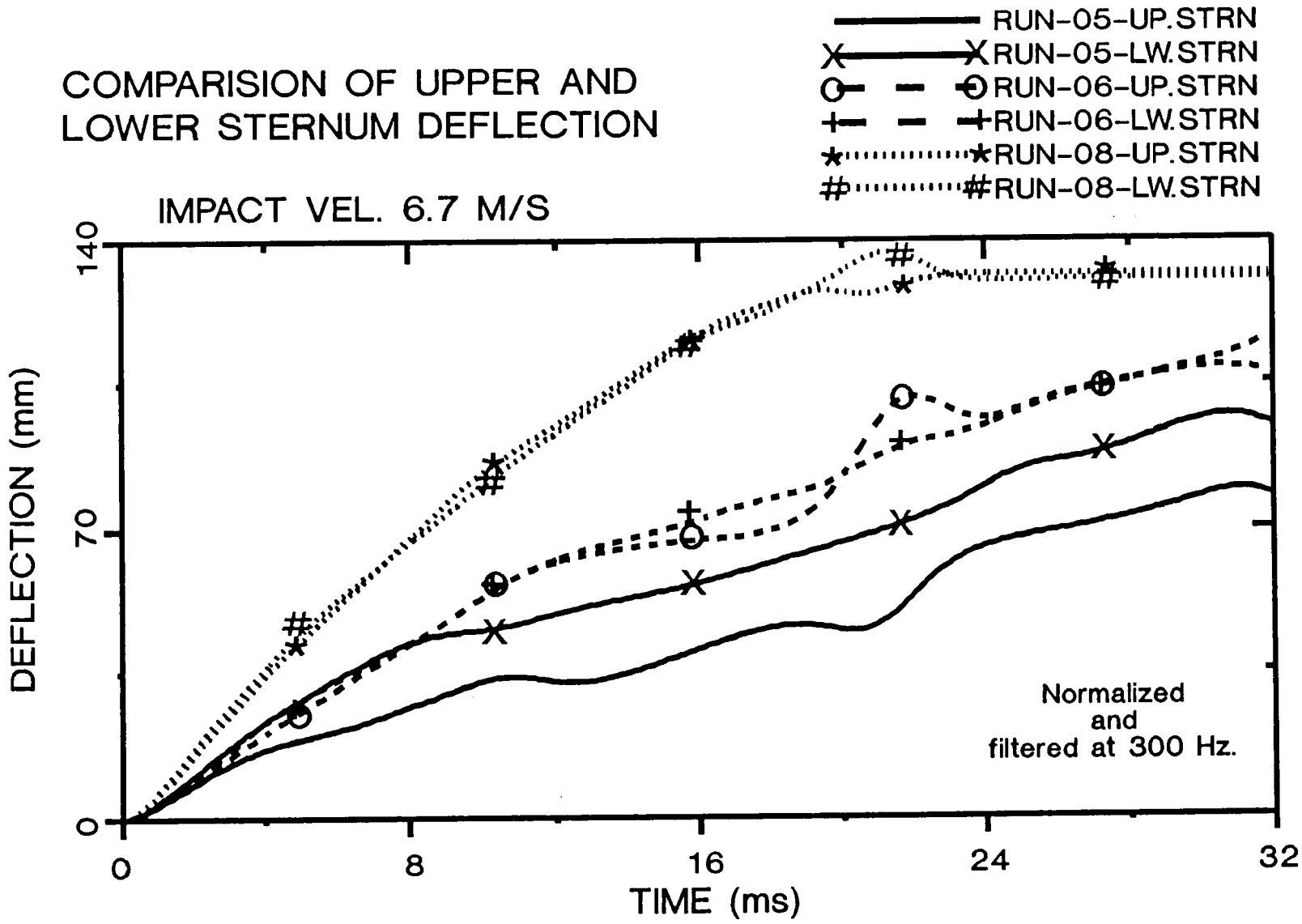

Wayne State University
Bioengineering Center

FIGURE A14

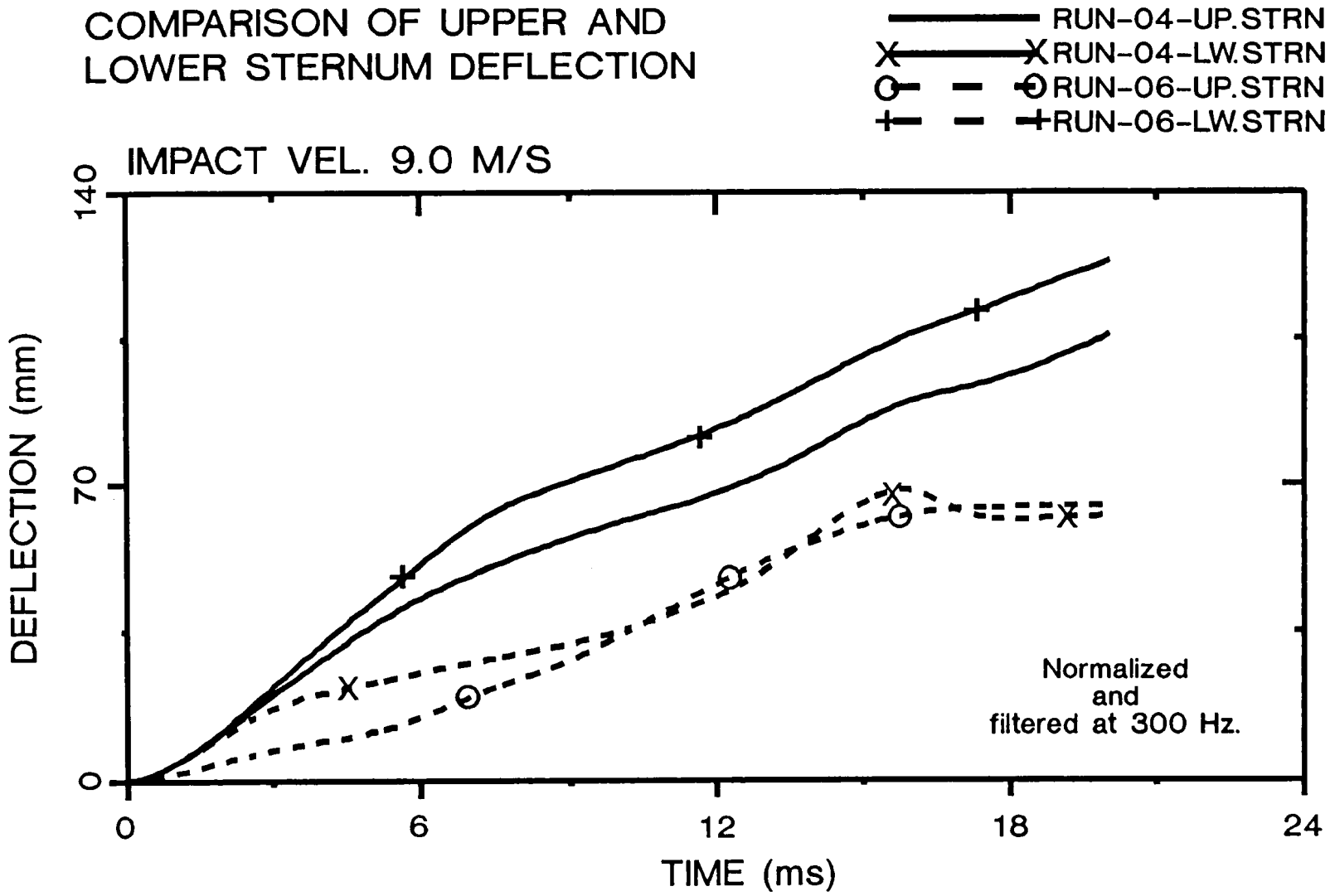

Wayne State University
Bioengineering Center

FIGURE A15

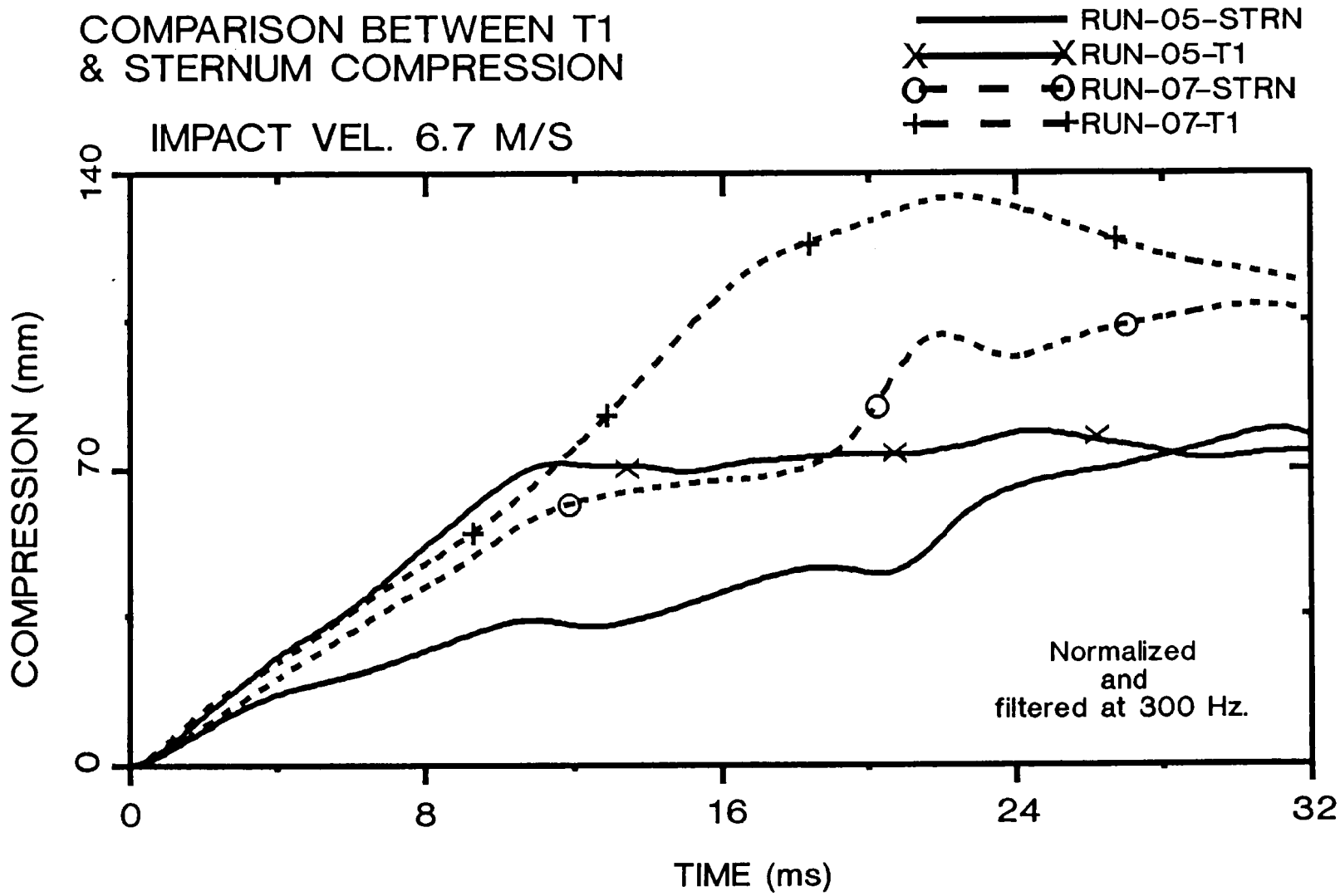

Wayne State University
Bioengineering Center

FIGURE A16

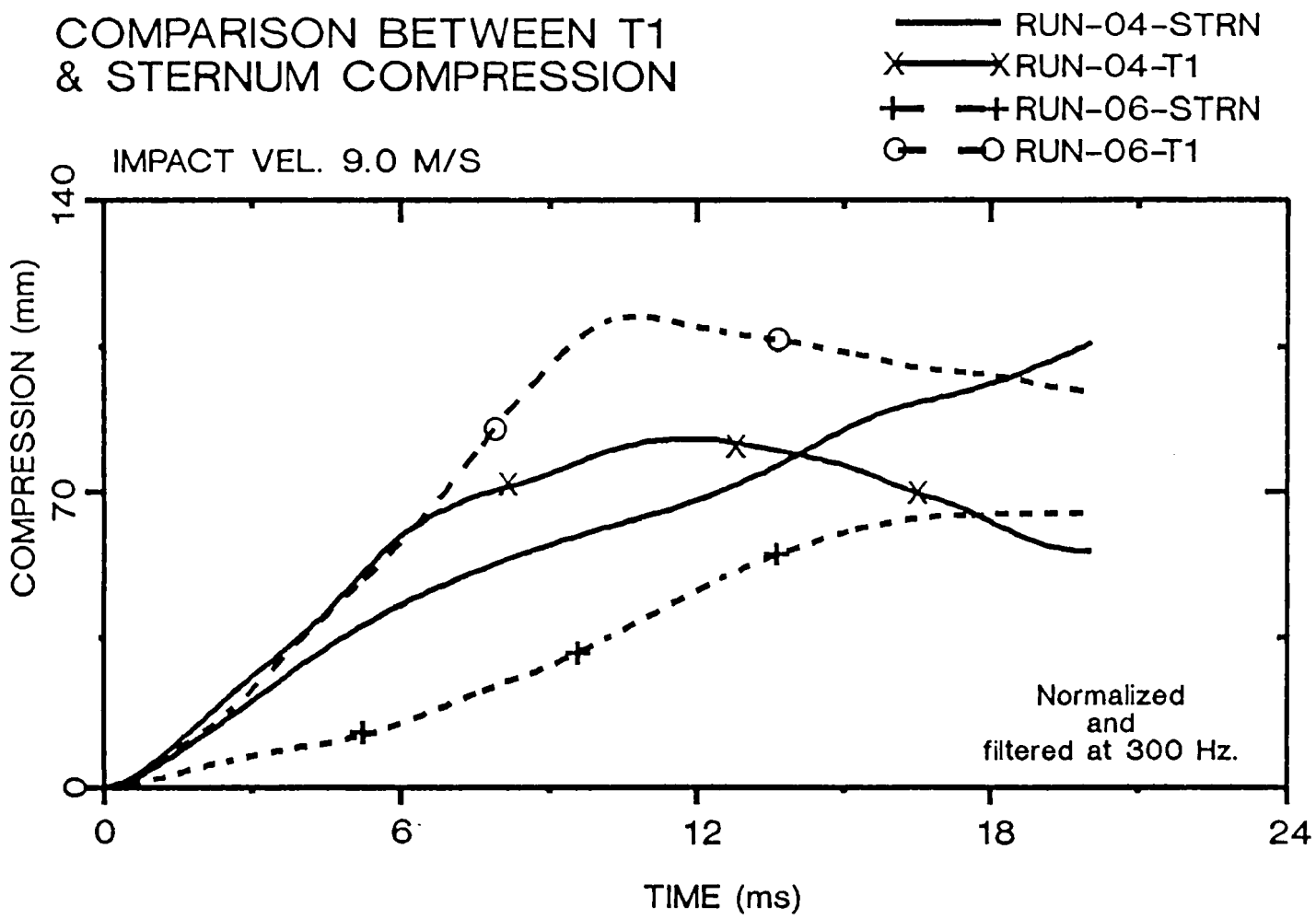

Wayne State University
Bioengineering Center

FIGURE A17

PAPER: TWO DIMENSIONAL ANALYSIS OF THE SHOULDER DUE TO LATERALLY APPLIED LOAD

SPEAKER: Tim Walilko, Wayne State University, Bioengineering Center

No Questions asked.